Materials Today • Volume xxx, Number xx • xxxx 2021 RESEARCH

RESEARCH: Original Research

Strongly enhanced electromechanical coupling in atomically thin transition metal dichalcogenides

Md Farhadul Haque [1], Peter Snapp [1], Jin Myung Kim [2], Michael Cai Wang [1,3], Hyung Jong Bae [1], Chullhee Cho [1], SungWoo Nam [1,2,*]

[1] Department of Mechanical Science and Engineering, University of Illinois at Urbana-Champaign, IL 61801, USA
[2] Department of Materials Science and Engineering, University of Illinois at Urbana-Champaign, IL 61801, USA
[3] Department of Mechanical Engineering, University of South Florida, FL 33620, USA

Flexoelectricity in thin films has emerged as an effective electromechanical response owing to appealing scaling law and universal existence. However, current studies show limited out-of-plane converse flexoelectric effect (CFE) of ultra-thin transition metal dichalcogenides (TMDs) when compared to their conventional in-plane piezoresponse. Here, we report converse flexoresponse of atomically thin TMDs such as molybdenum disulfide (MoS_2) and tungsten diselenide (WSe_2) which exceeds their intrinsic in-plane piezoresponses. Our piezoresponse force microscopy (PFM) measurements revealed strongly enhanced CFE of the atomically thin MoS_2 and WSe_2 than their bulk counterpart (~700% enhancement in MoS_2, ~400% enhancement in WSe_2). We observed an anomalous reduction in converse flexoresponse in the monolayer structure attributed to a puckering deformation. By inducing a built-in in-plane tension to reduce puckering, we estimated the CFE of monolayer WSe_2 to be 8.14 pm/V, the highest among the atomically thin TMDs.

Introduction

Micro- or nanoscale energy conversion or actuation requires strong electromechanical coupling in the constituent materials [1–8]. Piezoelectricity is the most explored electromechanical response found in materials. However, piezoelectricity occurs only in non-centrosymmetric crystals and therefore, exists in only 20 out of 32 crystal classes [9]. Flexoelectricity is another form of electromechanical response that exists in all crystal systems [10–12]. In flexoelectricity, materials deform in response to an inhomogeneous polarization such as induced by electric field (E-field) gradient, which is known as converse flexoelectric effect (CFE). The lucrative scaling law (E-field gradient ~ 1/thickness^2) has motivated exploring flexoresponse at nanoscale [13,14]. Furthermore, enhanced electromechanical actuation has been demonstrated in nanoscale structures of three-dimensional materials compared to their bulk counterparts due to large "free surface" effect [15,16]. Exploiting this free surface could also augment the flexoresponse at the nanoscale.

Two dimensional (2D) transition metal dichalcogenides (TMDs), such as monolayer molybdenum disulfide (MoS_2) and tungsten diselenide (WSe_2), have been extensively explored to harness electromechanical responses [4,17], owing to their in-plane piezoresponse [18,19]. However, TMDs do not possess out-of-plane piezoelectricity due to inversion symmetry. Despite this, recent studies have reported CFE enabled out-of-plane electromechanical response (d_{33}) in monolayer TMDs on gold substrate [20]. Still, the measured d_{33} was smaller than the in-plane piezoresponse, possibly due to strong affinity between the gold substrate and overlaid chalcogen atoms [21]. Furthermore, probing d_{33} of monolayer TMDs on flexible plastic substrates [22] could expose the in-plane piezoresponse of the TMDs to the out-of-plane direction through substrate deformation (e.g., bending). However, the measured response cannot rigorously be

* Corresponding author.
E-mail address: Nam, S. (swnam@illinois.edu)

 https://doi.org/10.1016/j.mattod.2020.12.021

Please cite this article in press as: M.F. Haque et al., Materials Today (2021), https://doi.org/10.1016/j.mattod.2020.12.021

attributed to flexoelectricity due to the crosstalk between the in-plane and out-of-plane electromechanical response. Probing converse flexoelectricity without any extraneous effect is critical to study this universal yet underappreciated phenomenon in 2D TMDs.

In this work, we investigated the out-of-plane CFE (d_{33}) of MoS_2 and WSe_2 on silicon (Si) using piezoresponse force microscopy (PFM). First, we compared the CFE with the intrinsic in-plane piezoresponse. Our PFM measurements revealed stronger out-of-plane CFE than the in-plane piezoresponse. Second, we carried out detailed measurements to investigate the layer dependence on CFE. We observed 700% (MoS_2) and 400% (WSe_2) enhancement in CFE as the thickness reduced from bulk to the atomically thin limit. Third, we used a finite element analysis (FEA) to study the potential deformation mechanism dictated the CFE in PFM measurements. Our FEA study suggested that a potential puckering occurred during PFM measurement could attenuate the electric field gradient by an order of magnitude. Finally, we studied the effect of in-plane strain on the CFE. We proposed that in-plane tensile strain could reduce puckering and thereby increasing the CFE by ~46%. We reported CFE of monolayer WSe_2 to be ~8.14 pm/V, the highest electromechanical response reported for any monolayer TMDs.

Results and discussion

To prepare atomically thin TMDs samples for PFM characterizations, we transferred the mechanically exfoliated MoS_2 and WSe_2 onto highly-doped silicon (Si) substrates by wet transfer method (Material and Methods and Section 1, Supplementary Material). PFM was used to measure the out-of-plane displacement in response to an out-of-plane bias (Fig. 1a, Material and Methods and Section 2, Supplementary Material). The applied bias rapidly decays away from the atomic force microscope (AFM) tip (Fig. 1a inset), which results in an E-field gradient in concert with Si substrate serving as a ground electrode. The resultant deformation due to E-field gradient was measured as a function of applied AC voltage (V_{ac}), where deformation = $d_{33} \times V_{ac}$. We then estimated d_{33} from the slope of the amplitude (i.e., deformation) vs. applied AC bias plot (Fig. 1b). Since TMDs do not possess out-of-plane piezoresponse, the origin of d_{33} was attributed to the CFE (Section 2 and 5, Supplementary Material).

Comparison between flexoresponse and piezoresponse

To decouple flexoelectricity from piezoelectricity, we began our measurement by characterizing bilayer MoS_2 (2L-MoS_2) with in-plane inversion symmetry. The d_{33} of 2L-MoS_2 was 4.92 pm/V (Fig. 1b) and is ~500% higher than the previously reported d_{33} of monolayer MoS_2 (1L-MoS_2, ~1 pm/V) [23]. The substrate (Si) exhibited negligible d_{33} (0.36 pm/V, Fig. 1b). We note that our estimated d_{33} is 167% higher than the in-plane piezoresponse (d_{11}) of 1L-MoS_2 (1.84 pm/V) [18,23]. We attribute the large d_{33} to the optimized substrate selection and measurement technique. Silicon demonstrated reduced interaction which allowed the MoS_2 atoms to more freely stretch towards the out-of-plane direction [24]. The large d_{33} is also attributed to the high signal to noise ratio enabled by the resonance-enhanced PFM measurement technique adopted in the current study [25].

We then estimated the d_{33} of 1L-MoS_2 and 1L-WSe_2 (Fig. 2a). Our d_{33} for 1L-MoS_2 (2.78 pm/V) and 1L-WSe_2 (5.55 pm/V) on Si are significantly larger than the previously reported d_{33} of 1L-MoS_2 (0.94 pm/V) and 1L-WSe_2 (0.43 pm/V) on gold substrate [20]. Furthermore, the d_{33} of both monolayer MoS_2 and WSe_2 are comparable or higher than the in-plane piezoresponse from previous literature (Fig. 2b) [19,23]. In the case of 1L-MoS_2, d_{33} exceeded d_{11} (1.84 pm/V) by 50%, whereas 1L-WSe_2 exhibited similar d_{33} compared to the d_{11} (5.1 pm/V). Despite the existence of non-zero d_{11} for 1L-TMDs, we can rule out any crosstalk between d_{11} and d_{33} since the atomically flat Si substrate prevented unwanted exposure of the in-plane to the out-of-plane direction. To the best of our knowledge, this is the first demonstration that the electromechanical response of TMDs induced by the out-of-plane CFE surpasses the conventional in-plane piezoresponse.

To compare the out-of-plane electromechanical response (d_{33}) with the in-plane response under same experimental conditions, we performed lateral PFM measurements on 1L-MoS_2 and 1L-

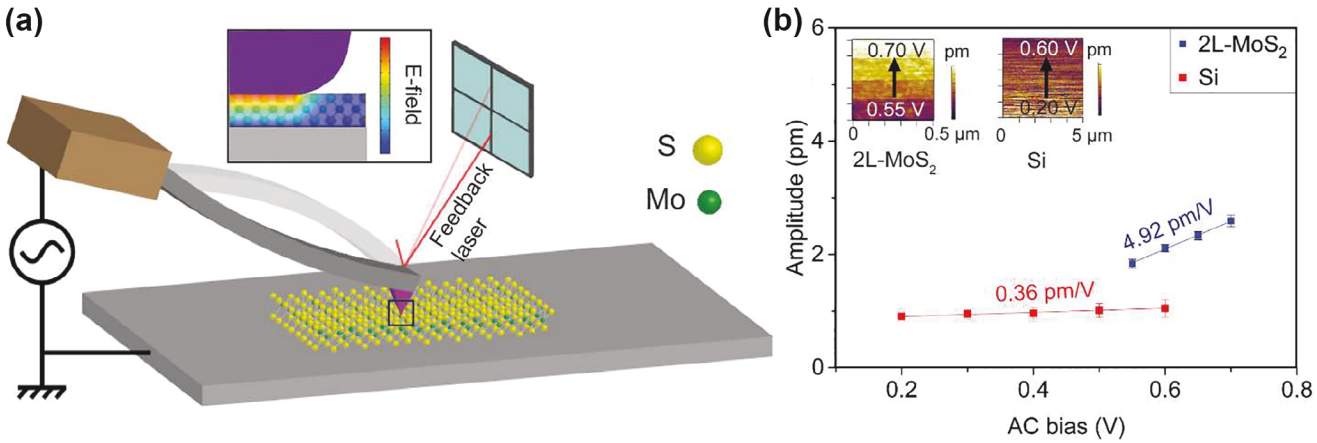

FIGURE 1

Converse flexoelectric effect of bilayer MoS_2. (a) Schematic drawing of the PFM measurement technique. The inset corresponds to generated E-field during PFM measurement. (b) Correlation between the applied AC bias and resulting PFM amplitude on bilayer MoS_2 and Si. PFM amplitude images of MoS_2 and Si under spatially modulated bias are shown in the inset. The error bars denote one standard deviation.

Please cite this article in press as: M.F. Haque et al., Materials Today (2021), https://doi.org/10.1016/j.mattod.2020.12.021

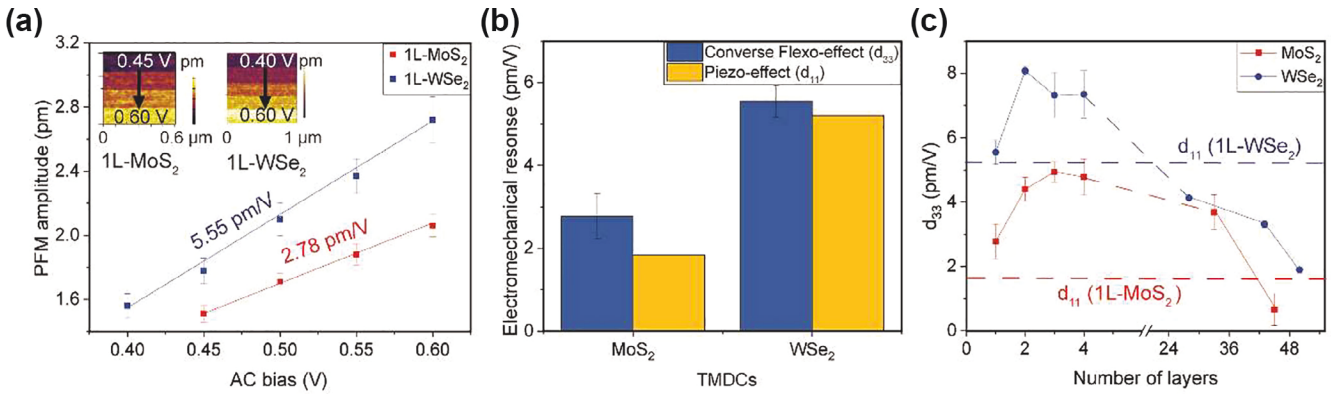

FIGURE 2

d_{33} measurement of different layers of MoS_2 and WSe_2. (a) PFM responses of monolayer MoS_2 and WSe_2. The corresponding PFM amplitude images are shown in the inset. (b) Out-of-plane flexoelectric, d_{33} of monolayer MoS_2 and WSe_2 measured in the present study compared to reported values of the in-plane piezoelectric coefficient, d_{11} [19,23]. (c) d_{33} trend with the number of layers of MoS_2 and WSe_2. The d_{11} of monolayer MoS_2 and WSe_2 are shown as horizontal dotted lines. The error bars denote one standard deviation.

WSe_2 (Fig. S1). The estimated in-plane piezorespone was 1.54 pm/V (MoS_2) and 3.46 pm/V (WSe_2), which are smaller than the literature values [19,23]. We note that the difference in substrate interaction might affect the in-plane deformation, resulting in a different in-plane piezorespone compared to the literature value.

Layer dependence of converse flexoelectric effect (d_{33})

To investigate the effect of the number of TMDs layers on CFE, we compared PFM scans of atomically thin (1–4 layer) and thick multilayer (>25 layers) MoS_2 and WSe_2 (Figure S2 and S3). We observed that atomically thin TMDs exhibit larger d_{33} than their bulk counterparts (Fig. 2c); ~700% larger in the case of MoS_2 (4.92 pm/V of 2L vs. 0.67 pm/V of >25 layers) and ~400% larger in the case of WSe_2 (8.08 pm/V of 2L vs. 1.9 pm/V of >25 layers). This large enhancement in d_{33} from atomically thin TMDs suggests that increased availability of free surface enhances CFE [15,16]. The free surface may allow the atomically thin material to 'stretch' the atomic bond length compared to the bulk state under E-field gradient. The evolution in d_{33} as thinning down the materials to the atomically thin limit clearly demonstrates that converse flexoelectricity induced electromechanical response can be enhanced in low dimensional systems.

Furthermore, we carried out a detailed examination of how varying the number of MoS_2 and WSe_2 layers in the atomically thin limit (1–4 layers) influences d_{33} (Fig. 2c). For both MoS_2 and WSe_2, we observed a significant increase in d_{33} moving from monolayer to bilayer (2.78 pm/V vs. 4.4 pm/V for MoS_2, 5.55 pm/V vs. 8.08 pm/V for WSe_2). In contrast, comparing d_{33} between 2, 3, and 4 layers of MoS_2 and WSe_2, we observed minimal variation in d_{33} with added layers. This reduction of d_{33} in the monolayer compared to the 2–4 layers contradicts our hypothesis that increased free surface results in enhanced CFE.

Deformation mechanism of converse flexoelectric effect

To explain the anomalous reduction in d_{33} of 1L-TMDs, we investigated converse flexoelectricity induced deformation mechanisms. Two potential mechanical effects, bending (Fig. S4a) and puckering (Fig. S4b) induced delamination, can perturb d_{33}. As the likelihood of bending scales inversely with bending stiffness which increases with the number of TMD layers (Section 3, Supplementary Material), one would expect higher deformation of thinner TMDs under PFM characterization. In contrast, puckering induced delamination of the TMDs occurs at the leading edge of the AFM tip in contact with TMDs [26], aided by low bending stiffness, high tip-sample adhesion and high tip-sample friction. Therefore, to fully understand the susceptibility to pucker, one must consider bending stiffness, tip-sample adhesion/stiction and friction.

To investigate the susceptibility to bend or pucker, we carried out detailed analysis on bending stiffness of the atomically thin film, tip-sample adhesion and friction. We first analyzed the trends in d_{33} with bending stiffness. For bending stiffness, we considered both continuum plate (stiffness ~ thickness^3) and frictionless layer (stiffness ~ thickness) models (Fig. 3a) [27]. The d_{33} was minimum on the monolayer with minimal variation for the subsequent layers as a function of stiffness. Second, we measured the tip-sample adhesion force of monolayer and few layers MoS_2 and WSe_2 (Fig. 3b). We observed ~35.5% drop in the tip-adhesion force from monolayer to bilayer MoS_2 and ~24% drop for the WSe_2. Compared to the steep drop from monolayer to bilayer, the reduction in tip-sample adhesion was less apparent for 2–4 layers (20% for MoS_2, 13% for WSe_2). Third, a similar trend was observed in tip-sample friction force (Fig. 3c) of monolayer and few layers MoS_2, revealed by friction force microscopy. The sliding tip-sample friction dropped by 60% on the bilayer structure compared to the monolayer structure and saturated on the subsequent layers. The lowest d_{33} observed on the monolayer (Fig. 3a) rules out bending induced delamination as an explanation for enhanced d_{33} in multilayer samples. However, the significant drop in tip-sample adhesion and friction from monolayer to bilayer structure, followed by a saturation behavior on the next few layers (Fig. 3b and 3c) suggests that puckering induced delamination is most favorable on monolayer structure. We ruled out the susceptibility of the top layer to pucker for multilayer TMDs by considering layer dependent van der Waals interaction (Section 4, Supplementary Material).

Please cite this article in press as: M.F. Haque et al., Materials Today (2021), https://doi.org/10.1016/j.mattod.2020.12.021

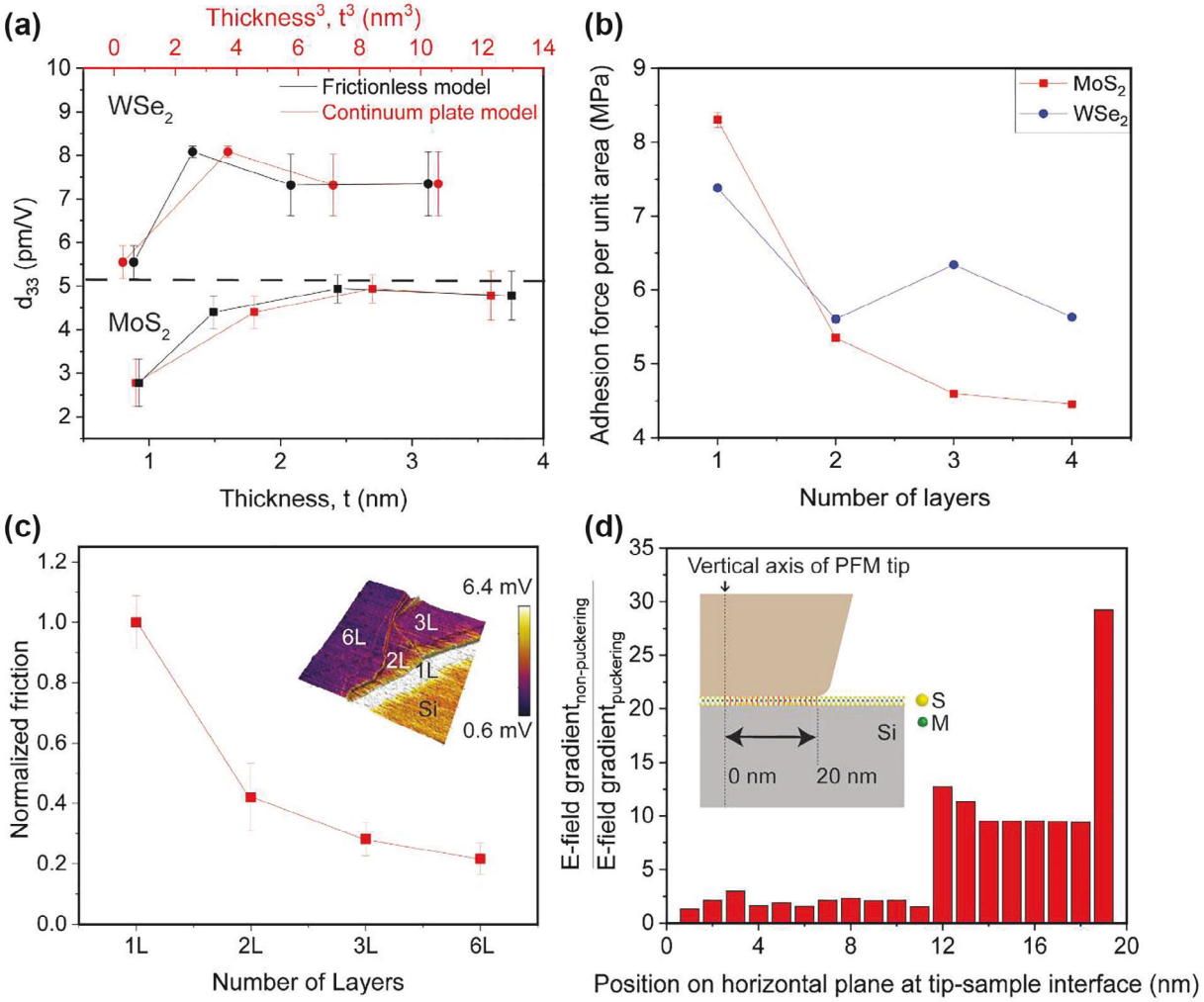

FIGURE 3

Investigation of possible deformation mechanisms in PFM measurement. (a) d_{33} trend with bending rigidity of the thin films, considering both frictionless layer model and continuum plate model [27]. MoS_2 and WSe_2 are separated by a horizontal dashed line. (b) Comparison of tip-sample adhesion force of MoS_2 and WSe_2 samples with different numbers of layers. (c) Sliding friction between the PFM tip and MoS_2 during PFM measurement as a function of the number of MoS_2 layers. The inset shows the friction force mapped on the topography. All the error bars denote one standard deviation. (d) The ratio of E-field gradient of the non-puckered structure to the puckered structure as a function of position under the AFM tip. The center of the AFM tip corresponds to 0 nm.

Next, to quantify the effect of puckering on CFE, we developed a finite element model of the E-field on puckered and non-puckered 1L-MoS_2 (Section 5, Supplementary Material) and extracted the E-field gradient as a function of the position under the AFM tip (Fig. 3d). Our simulation result shows an order of magnitude increase in the E-field gradient near the tip-sample leading edge when puckering was absent. We estimated that the E-field gradient of at least one-third of tip-sample contact area towards the leading edge would be affected by the puckering. Therefore, we attribute the reduction of monolayer d_{33} to puckering induced E-field gradient reduction.

The degree of puckering can be increased by any topographic feature since any unwanted wrinkles/blisters can increase the tip-sample contact area and therefore, increase puckering. The topography of 1L-WSe_2 and 2L-WSe_2 prepared by the wet transfer process show nanoscale wrinkles/blisters and intercalated particles (Fig. S5). We chose the PFM scan areas far away from the wrinkles/particles to avoid any effect from the unintended surface roughness induced by the particles. Furthermore, to avoid such features in microscale, we prepared another set of 1L- and 2L- WSe_2 samples by direct exfoliation on Si. Directly exfoliated WSe_2 showed no wrinkles/blisters (Fig. S5). The surface roughness of wet transfer and direct exfoliation samples used in our PFM study exhibited similar flatness level (~1.15–1.5 Å, Fig. S6 and Section 6, Supplementary Material). The flatness of the topography suggests that the effect of wrinkles/bubbles/particles to our PFM measurement is minimal.

Effect of strain on d_{33}

Although the wet transferred and directly exfoliated WSe_2 show similar surface roughness, the absence of wrinkles/blisters in directly exfoliated WSe_2 suggests that different levels of strain may exist between wet transferred and directly exfoliated WSe_2. The difference in strain level was confirmed by photoluminescence (PL) spectroscopy (Fig. S7). Based on the PL spectra [28,29], we estimated a ~0.4% in-plane tensile strain on directly

Please cite this article in press as: M.F. Haque et al., Materials Today (2021), https://doi.org/10.1016/j.mattod.2020.12.021

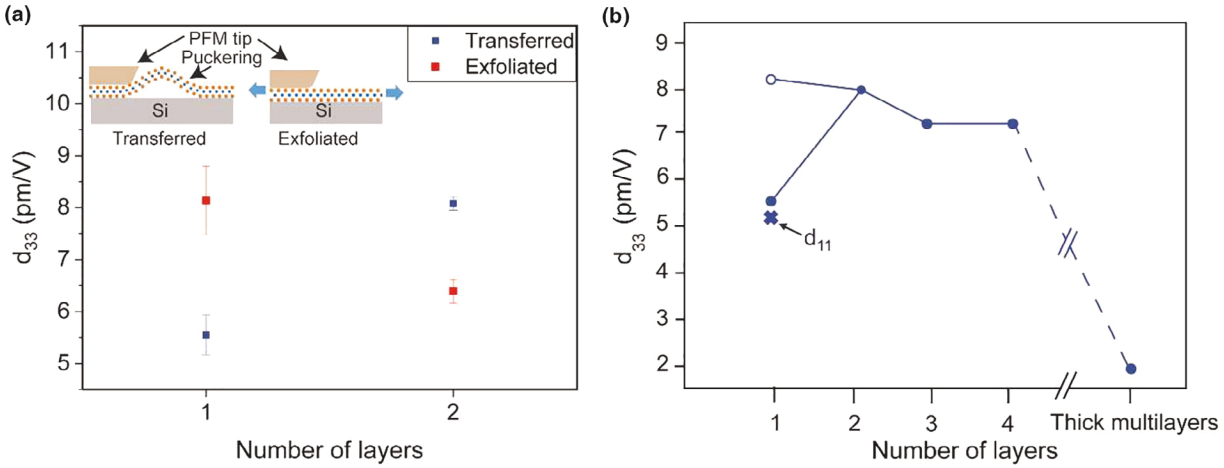

FIGURE 4

Effect of reduced puckering on d_{33}. (a) d_{33} measured on wet transferred (denoted as "Transferred") and directly exfoliated (denoted as "Exfoliated") WSe_2 on Si. The schematics of the monolayer structures with and without in-plane tension are shown in the inset. The error bars denote one standard deviation. (b) Comparison of d_{33} measured in this work with the literature value of in-plane piezoelectric coefficient (d_{11}) of WSe_2 monolayer (shown as a cross). The enhanced d_{33} of exfoliated WSe_2 monolayer is shown as a hollowed circle.

exfoliated 1L-WSe_2 and ~0.75%-1% in-plane tensile strain for directly exfoliated 2L-WSe_2 compared to their wet transferred counterpart (Section 7, Supplementary Material).

To investigate how in-plane tension affects d_{33}, we performed PFM scans on directly exfoliated WSe_2 (Fig. 4a and Fig. S8). Directly exfoliated 1L-WSe_2 on Si showed a 46% enhancement in d_{33} (8.14 pm/V) compared to wet transferred 1L-WSe_2 (5.55 pm/V). In contrast, the d_{33} of directly exfoliated 2L-WSe_2 (6.39 pm/V) showed a 21% reduction compared to its wet transferred (8.08 pm/V) counterpart (Fig. 4a). The enhancement in d_{33} of directly exfoliated 1L-WSe_2 suggests that in-plane tension facilitated the reduction in puckering. However, the reduced d_{33} for directly exfoliated 2L-WSe_2 suggests careful balancing of reduced puckering and in-plane tension is necessary to maximize d_{33}. The bilayer structure (wet transferred or directly exfoliated) would experience much less puckering compared to the monolayer structure due to high bending stiffness, reduced tip-sample adhesion (Fig. 3b) and reduced friction (Fig. 3c). Therefore, we hypothesize that both the directly exfoliated and wet transferred 2L-WSe_2 experienced similar degree of minimal puckering. However, the in-plane tension (~0.75%–1%) present in directly exfoliated 2L-WSe_2 restricts the out-of-plane deformation, resulting in a reduced d_{33}. Such restricted deformation due to ~0.4% in-plane tension could also be present in directly exfoliated 1L-WSe_2. Nonetheless, the d_{33} of directly exfoliated 1L-WSe_2 yielded the highest CFE (8.14 pm/V) among all the monolayer TMDs studied to date (Fig. 4b). Balancing the anti-puckering and restricted deformation due to in-plane tension might further enhance the d_{33} of monolayer TMDs.

Conclusion

We demonstrated strong CFE (d_{33}) in monolayer MoS_2 and WSe_2 which outperforms their intrinsic in-plane piezoresponse (d_{11}). Furthermore, we showed that the thinning down of MoS_2 and WSe_2 to the atomic layers enhances the CFE relative to their bulk counterpart. We observed reduced d_{33} of monolayer MoS_2 and WSe_2 compared to 2–4 layers which were attributed to increased puckering of monolayer structure which dampens the E-field gradient. By introducing a flatter topography to counter puckering, we observed that 1L-WSe_2 demonstrated a larger out-of-plane deformation relative to puckered samples. This work represents the first demonstration that reducing the thickness of TMDs to the atomic limit enhances the flexoelectric out-of-plane displacement to the point of surpassing the in-plane piezoelectric response. The converse flexoelectricity observed in the atomically thin TMD is comparable to the piezoresponse of commercially available bulk materials and multilayer Janus TMD systems [30,31], thereby establishing flexoelectricity as an exciting phenomenon for nanoscale actuation or energy harvesting applications. In addition, given the growing interest in stacking and twisting various TMDs [32], the control of stacking order and twist angle of multilayer TMDs might allow further modulation of converse flexoelectric effect. We expect that our findings will enable the application of flexoelectric atomically thin materials as next-generation nanoscale energy conversion and actuation systems.

Material and methods

Sample preparation

The MoS_2 and WSe_2 used in this study were mechanically exfoliated from commercially available bulk crystals (HQ Graphene) on SiO_2/Si substrates, followed by a wet transfer process (Fig. S9). The SiO_2 was used as the sacrificial layer during the wet transfer process. Polymethyl methacrylate (PMMA) was used as a handling layer. Potassium hydroxide (15 wt%) solution was used at 80 °C to etch away the SiO_2 layer during the wet etching. Once the etching was completed, the material (with PMMA) was transferred on deionized water baths for several iterations to clean up any residual ions from the wet etching process. The material was then transferred onto the target substrate (silicon) followed by PMMA removal by acetone and standard degreasing. For the directly exfoliated WSe_2, the TMD was exfoliated on a Si

Please cite this article in press as: M.F. Haque et al., Materials Today (2021), https://doi.org/10.1016/j.mattod.2020.12.021

substrate. No wet etching was required for the direct exfoliation of WSe_2. Since all the multilayer TMDs were prepared by exfoliating from the bulk crystal without any manual rotation, we assumed that all the multilayer TMDs would exhibit lowest energy stacking order (AB stacking). Further details about the characterizations of the samples can be found in the Supplementary Material.

PFM measurement

To characterize the converse flexoelectric response of MoS_2 and WSe_2 at a sub-20 nm spatial resolution, we adopted the dual AC resonance tracking piezoresponse force microscopy (DART PFM) technique [25]. The resonance-enhanced PFM technique adopted in this study enables high signal to noise ratio characterization, which is essential to detect weak electromechanical responses. During PFM measurement (Fig. 1a), AC voltage is supplied to the metal coated cantilever (Budget Sensor Multi75E with 3 N/m force constant, platinum coated) which is brought in contact with the sample of interest. As the cantilever rasters along the surface with the oscillating bias applied to it, the sample oscillates due to piezoresponse (or flexoresponse). The oscillation of the sample due to piezoresponse (or flexoresponse) is recorded by the cantilever deflection via a lock-in amplifier. A standard PFM scan yields three images – topography, PFM amplitude and PFM phase. The vertical (lateral) deflection of the cantilever due to the oscillating bias is stored in the case of vertical (lateral) PFM. The amplitude contains information about the strength of the piezoresponse (or flexoresponse) or any other form of electromechanical response [33], whereas the phase shows the dipole direction and other forms of non-piezoelectric response [34]. The strength of the piezoresponse (or flexoresponse) is known as the piezoelectric coefficient and estimated from the linear correlation between the PFM amplitude and applied AC bias. In this study, the effective out-of-plane piezoelectric coefficient is addressed as d_{33}.

Data availability

The data that support all plots within this paper is available from the corresponding author upon reasonable request.

Author contributions

M.F.H. performed the sample preparation, PFM characterization and finite element analysis. J.M.K. and M.C.W. performed the sample preparation. S.W.N. initiated and oversaw the project. All authors contributed to the analysis of data and writing of the manuscript.

CRediT authorship contribution statement

Md Farhadul Haque: Investigation, Formal analysis, Data curation, Writing - original draft, Visualization. **Peter Snapp:** Formal analysis, Resources, Writing - review & editing. **Jin Myung Kim:** Resources, Formal analysis, Writing - review & editing. **Michael Cai Wang:** Resources, Formal analysis, Writing - review & editing. **Hyung Jong Bae:** Formal analysis, Resources, Writing - review & editing. **Chullhee Cho:** Formal analysis, Resources, Writing - review & editing. **SungWoo Nam:** Conceptualization, Supervision, Project administration, Funding acquisition, Writing - review & editing.

Declaration of Competing Interest

The authors declare that they have no known competing financial interests or personal relationships that could have appeared to influence the work reported in this paper.

Acknowledgments

This work was supported by ONR YIP (N00014-17-1-2830), NASA ECF (NNX16AR56G), NSF (MRSEC DMR-1720633, ECCS-1935775, CMMI-1554019, CMMI-1904216, and DMR-1708852), AFOSR (FA2386-17-1-4071), and KRICT (GO!KRICT KK1963-807). Sample preparation and PL characterization were performed at Holonyak Micro & Nanotechnology Lab, University of Illinois. The PFM characterization was carried out in part in the Material Research Laboratory Central Research Facilities, University of Illinois. This research was partially supported by the NSF through the University of Illinois at Urbana-Champaign Materials Research Science and Engineering Center DMR-1720633.

Appendix A. Supplementary data

Supplementary data to this article can be found online at https://doi.org/10.1016/j.mattod.2020.12.021.

References

[1] Y. Qi et al., Nano Lett. 11 (2011) 1331–1336.
[2] P.X. Gao et al., Adv. Mater. 19 (2007) 67–72.
[3] Z.L. Wang, J. Song, Science 312 (2006) 242.
[4] W. Wu et al., Nature 514 (2014) 470–474.
[5] M.D. Manrique-Juárez et al., Coord. Chem. Rev. 308 (2016) 395–408.
[6] S.H. Baek et al., Science 334 (2011) 958.
[7] R.H. Baughman et al., Science 284 (1999) 1340.
[8] K.Y. Ma et al., Science 340 (2013) 603.
[9] H. Zhou et al., Appl. Phys. Lett. 108 (2016) 101908.
[10] T. Dumitrică, C.M. Landis, B.I. Yakobson, Chem. Phys. Lett. 360 (2002) 182–188.
[11] S. Krichen, P. Sharma, J. Appl. Mech. 83 (2016).
[12] T.D. Nguyen et al., Adv. Mater. 25 (2013) 946–974.
[13] M.-M. Yang, D.J. Kim, M. Alexe, Science 360 (2018) 904.
[14] S.M. Park et al., Nat. Nanotechnol. 13 (2018) 366–370.
[15] H.J. Xiang et al., Appl. Phys. Lett. 89 (2006) 223111.
[16] X. Wang et al., Sci. Adv. 2 (2016) e1600209.
[17] J.-H. Lee et al., Adv. Mater. 29 (2017) 1606667.
[18] H. Zhu et al., Nat. Nanotechnol. 10 (2015) 151–155.
[19] E. Nasr Esfahani et al., Nano Energy 52 (2018) 117–122.
[20] C.J. Brennan et al., Appl. Phys. Lett. 116 (2020) 053101.
[21] M. Velický et al., ACS Nano 12 (2018) 10463–10472.
[22] J. Seo et al., Appl. Surf. Sci. 487 (2019) 1356–1361.
[23] C.J. Brennan et al., Nano Lett. 17 (2017) 5464–5471.
[24] J. Torres et al., Phys. Status Solidi A 215 (2018) 1700512.
[25] B.J. Rodriguez et al., Nanotechnology 18 (2007) 475504.
[26] C. Lee et al., Science 328 (2010) 76.
[27] E. Han et al., Nat. Mater. 19 (2020) 305–309.
[28] I. Niehues et al., Nano Lett. 18 (2018) 1751–1757.
[29] S.B. Desai et al., Nano Lett. 14 (2014) 4592–4597.
[30] A. Labuda, R. Proksch, Appl. Phys. Lett. 106 (2015) 253103.
[31] L. Dong, J. Lou, V.B. Shenoy, ACS Nano 11 (2017) 8242–8248.
[32] P. Rivera et al., Nat. Nanotechnol. 13 (2018) 1004–1015.
[33] D. Seol, B. Kim, Y. Kim, Curr. Appl. Phys. 17 (2017) 661–674.
[34] S.M. Neumayer et al., J. Appl. Phys. 128 (2020) 171105.

Please cite this article in press as: M.F. Haque et al., Materials Today (2021), https://doi.org/10.1016/j.mattod.2020.12.021